Immunization of Vγ2Vδ2 T cells programs sustained effector memory responses that control tuberculosis in nonhuman primates

Ling Shen[a,1], James Frencher[a,1], Dan Huang[a,1], Wandang Wang[a,1], Enzhuo Yang[a], Crystal Y. Chen[a], Zhuoran Zhang[a,b], Richard Wang[a], Arwa Qaqish[a], Michelle H. Larsen[c], Hongbo Shen[d,2], Steven A. Porcelli[c,e], William R. Jacobs Jr.[c,2], and Zheng W. Chen[a,2]

[a]Department of Microbiology and Immunology, Center for Primate Biomedical Research, University of Illinois College of Medicine, Chicago, IL 60612; [b]Department of Immuno-Oncology, Beckman Research Institute, City of Hope National Cancer Center, Duarte, CA 91010; [c]Department of Microbiology and Immunology, Albert Einstein College of Medicine, Bronx, NY 10461; [d]Clinic and Research Center of Tuberculosis, Shanghai Key Laboratory of Tuberculosis, Shanghai Pulmonary Hospital, Tongji University School of Medicine, Shanghai 200433, China; and [e]Department of Medicine, Albert Einstein College of Medicine, Bronx, NY 10461

Contributed by William R. Jacobs Jr., January 29, 2019 (sent for review July 12, 2018; reviewed by C. David Pauza and Frank A. W. Verreck)

Tuberculosis (TB) remains a leading killer among infectious diseases, and a better TB vaccine is urgently needed. The critical components and mechanisms of vaccine-induced protection against *Mycobacterium tuberculosis* (Mtb) remain incompletely defined. Our previous studies demonstrate that Vγ2Vδ2 T cells specific for (E)-4-hydroxy-3-methyl-but-2-enyl pyrophosphate (HMBPP) phosphoantigen are unique in primates as multifunctional effectors of immune protection against TB infection. Here, we selectively immunized Vγ2Vδ2 T cells and assessed the effect on infection in a rhesus TB model. A single respiratory vaccination of macaques with an HMBPP-producing attenuated *Listeria monocytogenes* (Lm *ΔactA prfA) caused prolonged expansion of HMBPP-specific Vγ2Vδ2 T cells in circulating and pulmonary compartments. This did not occur in animals similarly immunized with an Lm *ΔgcpE* strain, which did not produce HMBPP. Lm *ΔactA prfA** vaccination elicited increases in Th1-like Vγ2Vδ2 T cells in the airway, and induced containment of TB infection after pulmonary challenge. The selective immunization of Vγ2Vδ2 T cells reduced lung pathology and mycobacterial dissemination to extrapulmonary organs. Vaccine effects coincided with the fast-acting memory-like response of Th1-like Vγ2Vδ2 T cells and tissue-resident Vγ2Vδ2 effector T cells that produced both IFN-γ and perforin and inhibited intracellular Mtb growth. Furthermore, selective immunization of Vγ2Vδ2 T cells enabled $CD4^+$ and $CD8^+$ T cells to mount earlier pulmonary Th1 responses to TB challenge. Our findings show that selective immunization of Vγ2Vδ2 T cells can elicit fast-acting and durable memory-like responses that amplify responses of other T cell subsets, and provide an approach to creating more effective TB vaccines.**

tuberculosis | phosphoantigen | vaccine | HMBPP | γδ T cells

Tuberculosis (TB), caused by *Mycobacterium tuberculosis* (Mtb), is the leading killer among infectious diseases (1), largely due to the concurrent epidemic of HIV/AIDS and multidrug resistance (2–4). The current TB vaccine, bacillus Calmette–Guérin, protects young children from severe disseminated TB, but inconsistently protects against pulmonary TB in adults (5–11). Development of a better TB vaccine requires a deeper understanding of protective anti-TB components and mechanisms in humans (12). Recent clinical TB vaccine trials yielded both protective and unprotective results (13–15), while vaccine candidates against Mtb infection were actively tested in animal models (16–22). However, the protective components of the immune system and the mechanisms for enhanced vaccine protection remain poorly defined (23–26).

T cells expressing γδ T cell antigen receptors are a nonconventional T cell population (27–29). Studies carried out over several decades have addressed fundamental aspects of the major Mtb-reactive γδ T cell subset, Vγ2Vδ2 T cells, during TB and other infections (29–33). Vγ2Vδ2 T cells are the sole γδ T cell subset capable of recognizing the isoprenoid metabolites isopentenyl pyrophosphate (IPP) and microbial (E)-4-hydroxy-3-methyl-but-2-enyl pyrophosphate (HMBPP), which are usually referred to as phosphoantigens (34, 35). HMBPP is produced only by the nonmevalonate pathway present in some selected microbes, including Mtb and *Listeria*, whereas IPP can be produced by the mevalonate pathway in host cells (34, 35). HMBPP-specific Vγ2Vδ2 T cells exist only in humans and nonhuman primates (NHPs). They constitute 65–90% of total circulating human γδ T cells, contribute to both innate and adaptive immune responses in infections (36–39), and mount major expansion and

MICROBIOLOGY

Significance

Despite the urgent need for a better tuberculosis (TB) vaccine, relevant protective mechanisms remain unknown. We previously defined protective phosphoantigen (E)-4-hydroxy-3-methyl-but-2-enyl pyrophosphate (HMBPP)–specific Vγ2Vδ2 T cells as a unique subset in primates, and, here, we immunized them selectively for protection against TB. A single respiratory vaccination of macaques with attenuated HMBPP-producing *Listeria monocytogenes* (Lm *ΔactA prfA), but not an HMBPP-lacking *ΔgcpE Listeria* strain, expanded Vγ2Vδ2 T cells, elicited Th1-like Vγ2Vδ2 T cell responses, and reduced TB infection/pathology after moderate-dose TB challenge. Such protection correlated with rapid memory-like, Th1-like Vγ2Vδ2 T cell responses, the presence of tissue-resident Vγ2Vδ2 T effectors coproducing IFN-γ/perforin and inhibiting intracellular *Mycobacterium tuberculosis* growth, and enhanced $CD4^+/CD8^+$ T cell responses. These findings establish a concept incorporating immunization of human Vγ2Vδ2 T cells for TB vaccine development.**

Author contributions: L.S., J.F., D.H., W.W., M.H.L., H.S., W.R.J., and Z.W.C. designed research; L.S., J.F., D.H., W.W., E.Y., C.Y.C., Z.Z., R.W., A.Q., and H.S. performed research; M.H.L., W.R.J., and Z.W.C. contributed new reagents/analytic tools; L.S., J.F., D.H., W.W., E.Y., C.Y.C., Z.Z., H.S., S.A.P., W.R.J., and Z.W.C. analyzed data; and L.S., S.A.P., W.R.J., and Z.W.C. wrote the paper.

Reviewers: C.D.P., American Gene Technologies International, Inc.; and F.A.W.V., Biomedical Primate Research Centre.

The authors declare no conflict of interest.

[1]L.S., J.F., D.H., and W.W. contributed equally to this work.

[2]To whom correspondence may be addressed. Email: hbshen@tongji.edu.cn, william.jacobs@einstein.yu.edu, or zchen@uic.edu.

This article contains supporting information online at www.pnas.org/lookup/suppl/doi:10.1073/pnas.1811380116/-/DCSupplemental.

Published online March 8, 2019.

effector responses during infections with Mtb and other pathogens (29, 30, 31, 33, 40, 41). Recent seminal studies demonstrate that HMBPP plus IL-2 treatment of NHPs can specifically expand Vγ2Vδ2 T cells in vivo; following expansion, they are multifunctional and protective against infection with high doses of Mtb infection and other pathogens (29–33). Consistently, adoptive transfer studies showed that Vγ2Vδ2 T effector cells can traffic to and accumulate in the lungs as early as 6 h after transfer and attenuate Mtb infection in NHPs (42). Notably, rapid recall-like expansion of Vγ2Vδ2 T cells correlates with detectable immunity against fatal TB after Mtb challenge of bacillus Calmette–Guérin-vaccinated young rhesus macaques (29).

Protective features of Vγ2Vδ2 T cells raise the question of whether selective immunization of Vγ2Vδ2 T cells can elicit protective responses and induce immunity against Mtb infection. Proving this concept would be valuable for advancing our understanding of the role of these cells in immunity to infections, and would also provide a foundation for the development of new TB vaccines that include approaches to recruit protective Vγ2Vδ2 T cells in conjunction with other T cell subsets. To this end, we have employed an HMBPP-producing *Listeria monocytogenes* (Lm) vaccine vector for immunization of Vγ2Vδ2 T cells. While attenuated forms of Lm have been used as delivery systems to vaccinate humans against a variety of cancers (43), we combined *ΔactA* and *prfA** mutations to develop an attenuated but highly immunogenic vector (31, 44, 45). We have shown that Lm *ΔactA prfA** itself or its recombinants expressing various immunogens are highly attenuated and safe, eliciting remarkable expansion of Vγ2Vδ2 T effector cells after systemic or respiratory vaccination (46–49). In addition, recent studies, including ours, have shown that respiratory vector vaccination of NHP is safe and immunogenic (18, 20, 22, 48, 50). We therefore conducted a proof-of-concept study to test the hypothesis that respiratory Lm *ΔactA prfA** immunization of Vγ2Vδ2 T cells without concurrent immunization against other Mtb antigens can elicit protective effector memory responses and reduce Mtb infection in macaques. Our results showed that substantial protection was achieved by this approach.

Results

Expansion of HMBPP-Specific γδ T Cells by Immunization with HMBPP-Producing Lm *ΔactA prfA.** To target Vγ2Vδ2 T cells for vaccine design, we have employed an attenuated live Lm strain (Lm *ΔactA prfA**) that shares with Mtb the ability to produce HMBPP via the nonmevalonate pathway (44). We showed that respiratory or systemic immunization of macaques with this attenuated Lm *ΔactA prfA** strain or derivatives of this strain expressing microbial immunogens exhibited excellent safety profiles, elicited robust immune responses, and protected against life-threatening simian HIV-related malaria in macaques (31, 44, 46–48). We therefore used this vector for respiratory immunization of Vγ2Vδ2 T cells. The *ΔgcpE* deletion mutant of Lm *ΔactA prfA** served as a vector control, as this mutant no longer produced HMBPP due to the disruption of the gene *gcpE* encoding HMBPP synthase (48).

Intratracheal or respiratory vaccination of rhesus macaques with Lm *ΔactA prfA**, but not the *ΔgcpE* variant, elicited a prolonged expansion of HMBPP-specific Vγ2Vδ2 T cells in the circulation and airway [bronchoalveolar lavage (BAL) fluid; Fig. 1)]. At months 1–3 after vaccination, the Vγ2Vδ2 T cell subset increased and sustained up to almost 30% and 60% of total $CD3^+$ T cells in the blood (Fig. 1*A*) and airway (Fig. 1*B*), respectively.

Respiratory Lm *ΔactA prfA Vaccination Elicited Sustained Increases in Th1-Like Vγ2Vδ2 T Cells in the Airway.** IFN-γ plays a crucial role in anti-TB immunity, and also regulates multiple effector functions of Vγ2Vδ2 T cells (30, 32, 40, 42). We used intracellular cytokine staining (ICS) and flow cytometry to measure IFN-γ–producing Vγ2Vδ2 T cells in peripheral blood mononuclear cells (PBMCs) and in BAL fluid cells. To circumvent the issue of limited numbers of BAL fluid cells available for conventional

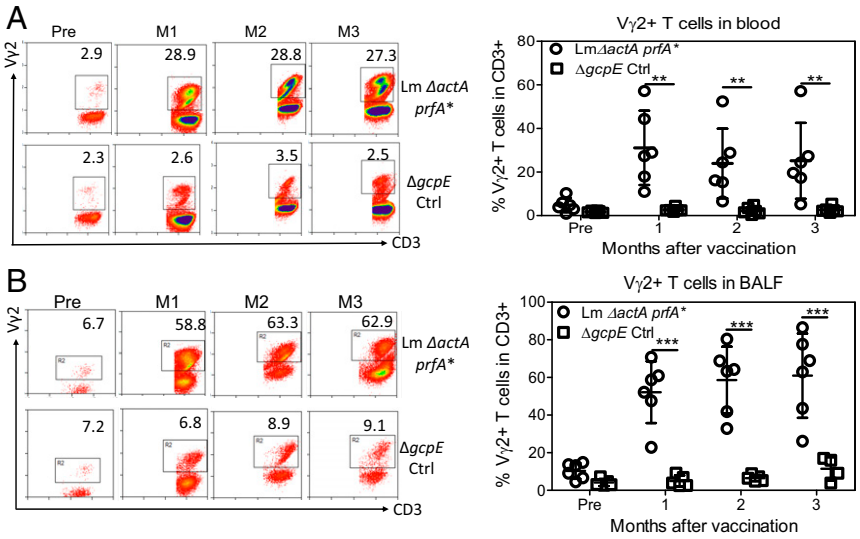

Fig. 1. Respiratory Lm *ΔactA prfA** immunization elicited prolonged expansion of Vγ2Vδ2 T cells in the lungs and blood. (*A*, *Left*) Representative flow cytometry histograms show percentages of $V\gamma2^+$ T cells in total $CD3^+$ T cells in blood at −0.5 mo (Pre) and at months (M) 1, 2, and 3 after respiratory vaccination of macaques with Lm *ΔactA prfA** (*Top*) and *gcpE* deletion mutant (*Bottom*; *ΔgcpE*) of Lm *ΔactA prfA**, respectively. Panels were gated on $CD3^+$ lymphocytes. Numbers in the upper right quadrant indicate the percentages of $V\gamma2^+$ T cells in the total $CD3^+$ T cell population. Expanded Vγ2 T cells are mostly Vδ2-coexpressing after Lm vaccination or primary TB infection, and therefore are interpreted as Vγ2Vδ2 T cells as described in previous publications (29–31). Ctrl, control. (*A*, *Right*) Dot plots with means ± SD representing expansions of Vγ2Vδ2 T cells for individual macaques per group before and 1–3 mo after the respiratory vaccination. (*B*) Representative flow cytometry histograms and graph of data as in *A*, except for cells from BAL fluid. Data in the graphs are dot plots with means ± SD of expansions for individual macaques per group. $*P < 0.05$; $** < 0.01$; $***P < 0.0001$ when comparing groups using a paired *t* test or Mann–Whitney *U* test. No *Listeria* could be isolated from the blood and BAL samples collected at indicated times from the vaccinated macaques as previously described (48).

ICS, we directly measured effector cells without prior antigen stimulation in culture using a direct ICS method that has been previously validated (31, 32, 49, 51–53). At 1 mo after respiratory Lm *ΔactA prfA** vaccination, about 10–20% of Vγ2Vδ2 T cells in BAL fluid samples were spontaneously producing IFN-γ without the need for HMBPP phosphoantigen stimulation in culture (*SI Appendix*, Fig. S1*A*). This high frequency of effector activity was maintained for at least 3 mo after the vaccination of macaques with Lm *ΔactA prfA**, but not the *ΔgcpE* control (*SI Appendix*, Fig. S1*A*).

Although direct ICS assay revealed much lower levels of IFN-γ^+ Vγ2Vδ2 T cells in the blood than we observed in the lungs (*SI Appendix*, Fig. S1*B*), the conventional ICS method with HMBPP stimulation in vitro allowed detection of ∼18–20% of IFN-γ^+ Vγ2Vδ2 T cells in the total blood $CD3^+$ T cells at 1 and 3 mo after the vaccination with Lm *ΔactA prfA**, but very low detection with the *ΔgcpE* control (*SI Appendix*, Fig. S1*C*).

Improved Control of Mtb Infection Following Vaccine-Induced Expansion Vγ2Vδ2 T Cells. We next sought to examine if the vaccine-elicited prolonged expansion of the Vγ2Vδ2 T effector subset led to detectable protection against Mtb challenge. To this end, macaques from groups immunized with Lm *ΔactA prfA**, the *ΔgcpE* vector control, or saline were challenged with 80 cfu of Mtb Erdman through bronchoscope-guided spread into the right caudal lung lobe at 12 wk after vaccination. Eighty colony-forming units of Mtb was considered a moderate–high dose for Chinese rhesus macaques (54). We assessed weight loss for vaccine effect, as it is a consistent clinical marker during primary active Mtb infection of macaques (42, 55). The γδ T cell-immunized group did not show an apparent weight loss over time (Fig. 2*A*). In contrast, vector and saline control groups exhibited significant losses of body weight after Mtb challenge (Fig. 2*A*).

Consistently, the γδ T cell-immunized macaques showed significantly lower Mtb colony-forming unit counts in the right caudal lung lobe (infection site), right middle lung lobe, and left lung lobe than those in both the vector and saline control groups at ∼2.5 mo after challenge (Fig. 2*B*, *Upper*; $P < 0.05$ and $P < 0.01$, respectively). Moreover, the γδ T cell-immunized animals also had limited extrapulmonary Mtb dissemination (Fig. 2*B*, *Lower*). Macaques in the γδ T cell-immunized group showed significant lower colony-forming unit counts in the spleen than those in the vector and saline control groups, respectively (Fig. 2*B*, *Lower*). Similarly, macaques in the γδ T cell-immunized group showed overall lower colony-forming unit counts in the liver or kidney tissues than animals in the vector and saline control groups (Fig. 2*B*, *Lower*). These results demonstrated that respiratory Lm *ΔactA prfA** immunization of Vγ2Vδ2 T cells conferred the ability to contain pulmonary Mtb infection and extrapulmonary dissemination after a pulmonary Mtb challenge.

Reduced Pathology in the Lung and Other Organs with Lm *ΔactA prfA Immunization of Vγ2Vδ2 T Cells.** We then evaluated TB pathology at ∼2.5 mo after challenge, as published studies show that TB pathology in the lungs can be well established at ∼2 mo after Mtb infection of NHPs (30, 42). Overall, vector and saline control groups exhibited similar severe TB pathology in lung, especially in the infection site in the right caudal lung lobe (Fig. 3*A*). Most of control animals (four or five in the vector or saline group) had TB pneumonia or miliary caseating lesions and extensive coalescing granulomas in the right caudal lobe and, to a lesser extent, in the right middle lobe (Fig. 3*A*). In addition, TB granulomas were often found in the opposite lung, mostly in the left caudal lobe (Fig. 3*A*; also reflected by the entire pathology scores in Fig. 3*B*). Notably, most control macaques exhibited disseminated TB granulomas in the spleen (as reflected by the entire scores in Fig. 3*B* and also shown in *SI Appendix*, Fig. S2*A*). Such TB dissemination was also seen in other extrapulmonary

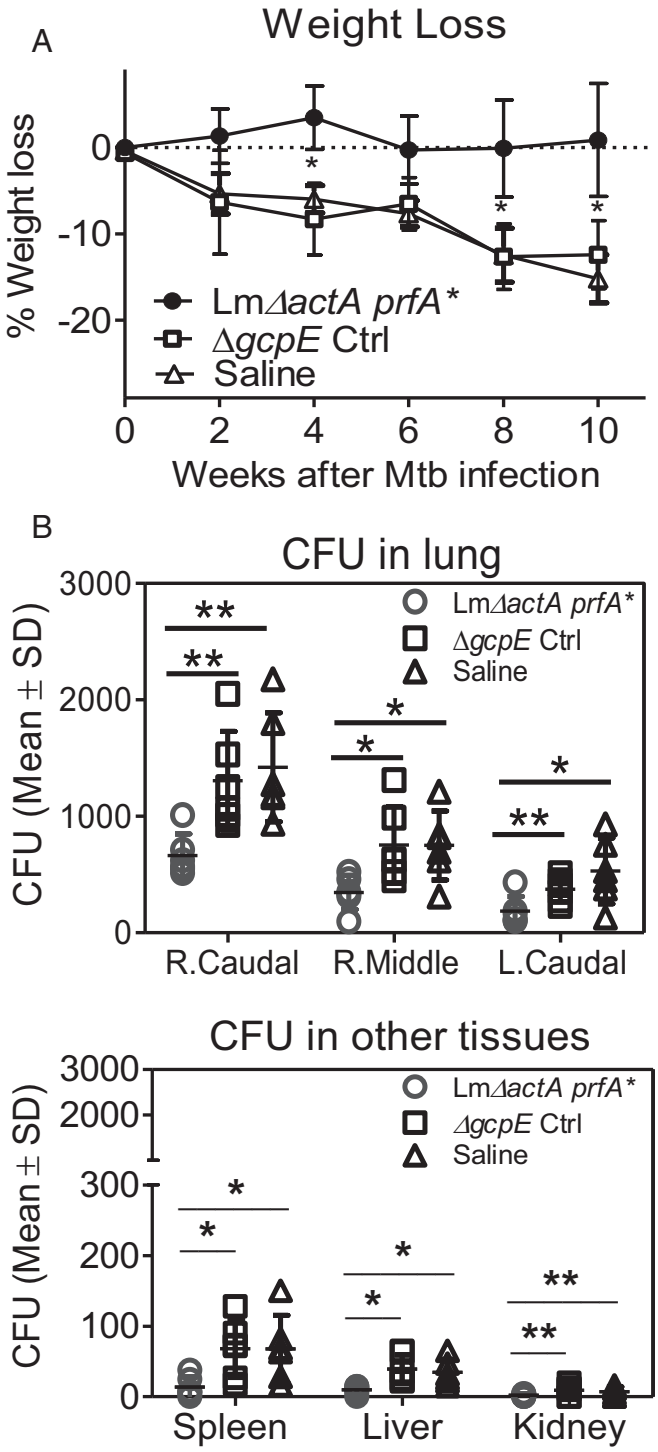

Fig. 2. Respiratory immunization of Vγ2Vδ2 T cells reduced tissue bacterial burdens after Mtb challenge. (*A*) Mean percentages of body weight loss in the three groups of macaques at indicated times after Mtb challenge. Note that body weights at post time points are subtracted by values at pre-infection for each of individuals before data analysis. Ctrl, control. (*B*) Bacterial burdens (colony-forming unit counts) in homogenized tissues. Mean colony-forming unit counts shown were from 1-cm^3 samples of different lung lobes as indicated (*Upper*) or from samples of extrapulmonary organs (*Lower*) collected at the time of necropsy. Dot plots in graph data represent colony-forming unit counts for individual macaques in each group with means ± SD. $*P < 0.05$; $**P < 0.01$ (Mann–Whitney *U* test and ANOVA).

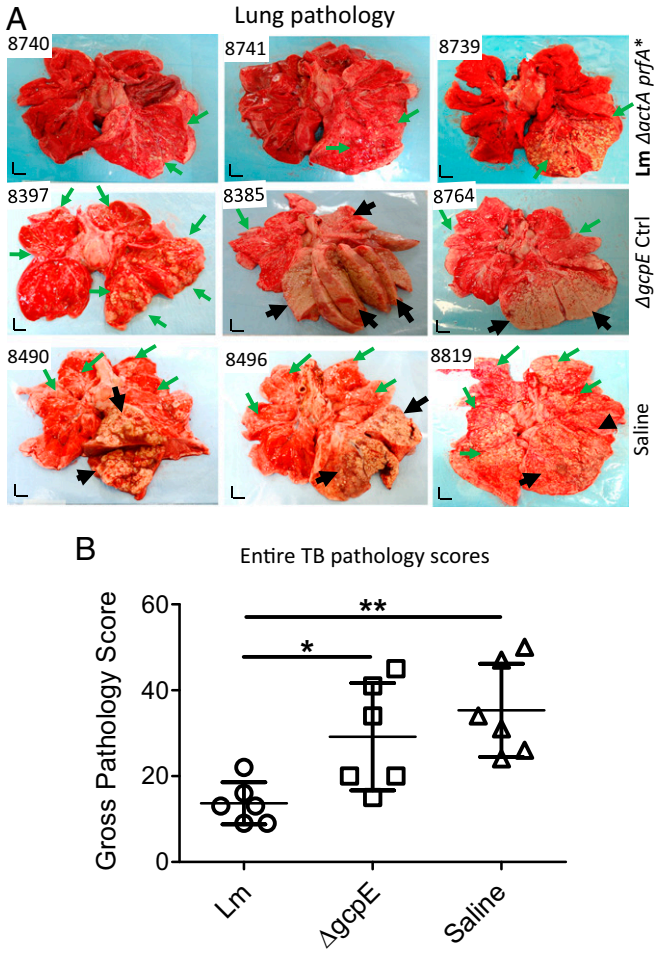

Fig. 3. Effect of respiratory Lm *ΔactA prfA** immunization on gross and microscopic pathology of the lungs. (*A*) Gross pathology of lungs from representatives of the test and control groups removed at necropsy ∼2.5 mo after Mtb challenge. The right caudal lung lobe, the Mtb infection site, is displayed in the bottom right portion of each photograph. Black arrows indicate caseation pneumonia or extensive coalescing granulomas. Green arrows demonstrate areas with fewer coalescing or noncoalescing granulomas. (Vertical and horizontal scale bars: 1 cm.) Overall, three representatives display relatively low, moderate, and high intensities of lesions as seen in each group. (*B*) Graph dot plots represent entire pathology scores for all individual macaques in each group. Pathology scores that we and other primate groups employ and publish actually include all of the subscores derived from each of the lung lobes and extrapulmonary organs. Pathology scoring of lungs and other organs was performed by a blinded pathologist. Data ranges for each group are shown as means ± SD. $*P < 0.05$, $**P < 0.01$ (Mann–Whitney *U* test and ANOVA). Microscopic pathology data are shown in *SI Appendix*, Fig. S2*B*.

organs as well as in the liver and kidney of most control macaques. In contrast, most macaques in the γδ T cell-immunized group did not show TB pneumonia or miliary TB caseating lesions or extensive coalescing granulomas, but generally exhibited less-coalescing or localized TB lesions limited to the infection site in the right caudal lobe (Fig. 3). Most macaques in the γδ T cell-immunized group did not show detectable gross TB granulomas in the spleen, liver, or kidney (as reflected by the entire pathology score in Fig. 3*B* and also shown in *SI Appendix*, Fig. S2*A*).

Comparison of the entire TB pathology between groups using established quantitative scoring criteria (19, 30, 42, 56) confirmed that the γδ T cell-immunized macaques had significantly milder TB lesions or pathology than the vector and saline control groups (Fig. 3*B*; $P < 0.05$ and $P < 0.01$, respectively). Overall, the macroscopic TB pathology lesions were consistent with the histopathological changes in lung sections derived from the right caudal lobe, middle lobes, and left caudal lobe (*SI Appendix*, Fig. S2*B*). Compared with the vector and saline control group macaques, the γδ T cell-immunized animals appeared to exhibit less necrotic and more lymphocytic granulomas, with fewer inflammatory macrophages, giant cells, or neutrophils infiltrating the granulomatous lesions (*SI Appendix*, Fig. S2*B*).

Rapid Recall of Th1-Like Vγ2Vδ2 T Cell Responses in the Airway After Mtb Challenge of Lm *ΔactA prfA-Vaccinated Macaques.** To establish immune correlates of protection against Mtb infection in Lm *ΔactA prfA**-vaccinated macaques, we investigated whether IFN-γ^+ Vγ2Vδ2 T cells coincided with protection against Mtb challenge. This was done using the direct ICS assay (as discussed above), which enabled us to use limited BAL fluid cells to assess how fast Vγ2Vδ2 T cell effector responses developed after pulmonary Mtb challenge. Surprisingly, as early as 10 d after Mtb challenge, IFN-γ^+ Vγ2Vδ2 T effector cells rapidly increased to the level of mean ∼40% of $CD3^+$ T cells within the lungs of Lm *ΔactA prfA**-vaccinated macaques (Fig. 4*A*). Pulmonary IFN-γ^+ Vγ2Vδ2 T cells in this group were maintained at ∼30% of total airway T cells on day 28 and, subsequently, at ∼20–30% on days 45 and 56, respectively (Fig. 4*A*). The sustained IFN-γ^+ Vγ2Vδ2 T cell response was consistent with the high frequency of Vγ2Vδ2 T cells in the airway (Fig. 4*B*). Blood IFN-γ^+ Vγ2Vδ2 T effector cells did not increase like those in the airway following Mtb challenge (*SI Appendix*, Fig. S3), which may have reflected the pulmonary migration of these circulating γδ T cells.

Inhibition of Intracellular Growth of Mtb by Vaccine-Induced Tissue-Resident Vγ2Vδ2 T Effector Cells. Our previous mechanistic studies showed that Vγ2Vδ2 T cells inhibited intracellular Mtb growth in an IFN-γ– and perforin-dependent fashion (30, 42). To determine whether Vγ2Vδ2 T cells coproducing IFN-γ and perforin, and capable of inhibiting intracellular Mtb, were detectable in the airway, lung, or lymphoid tissues after Mtb infection of vaccinated macaques, we used in situ confocal microscopic immune staining and ICS assays. With the in situ approach, appreciable numbers of IFN-γ^+ and perforin$^+$ Vγ2 T cells were detected in lung tissues from Lm *ΔactA prfA**-vaccinated macaques but not control animals (Fig. 5*A* and *SI Appendix*, Fig. S4). Consistently, the direct ICS assay revealed that the Lm *ΔactA prfA**-vaccinated rhesus macaque group showed approximately fivefold greater percentages of Vγ2Vδ2 T cells coproducing both IFN-γ and perforin in the airway compared with the vector control (Fig. 5*B*).

We then examined if greater numbers of IFN-γ– and perforin-coexpressing Vγ2 T cells in Lm *ΔactA prfA**-vaccinated animals were also associated with a stronger ability to inhibit Mtb growth in autologous macrophages (MΦ). Due to the limited availability of lymphocytes isolated from lungs, we evaluated IFN-γ and perforin coproduction as well as Mtb inhibition by resident Vγ2Vδ2 T cells in the spleen, which harbors large numbers of γδ T cells in rhesus macaques (57). Similar to the lungs, the numbers of IFN-γ– and perforin-coexpressing Vγ2 T cells were higher in spleens of Lm *ΔactA prfA**-vaccinated macaques than in the control group, regardless of HMBPP stimulation (Fig. 5*C*, *Left* and *Center*). When Vδ2 T cells were purified from spleens of the test or control group animals, we found that splenic Vδ2 T cells from the Lm *ΔactA prfA**-vaccinated group inhibited intracellular Mtb growth more potently in MΦ than did those from vector control animals (Fig. 5*C*, *Right*).

Rapid Recruitment of Conventional $CD4^+$/$CD8^+$ T Cells by Immunization of Vγ2Vδ2 T Cells. Given the multifunctional potential of Vγ2Vδ2 T cells (58), we examined whether Lm *ΔactA prfA**-induced Vγ2Vδ2 T cells could facilitate recruitment of αβ $CD4^+$ and $CD8^+$ T cells in

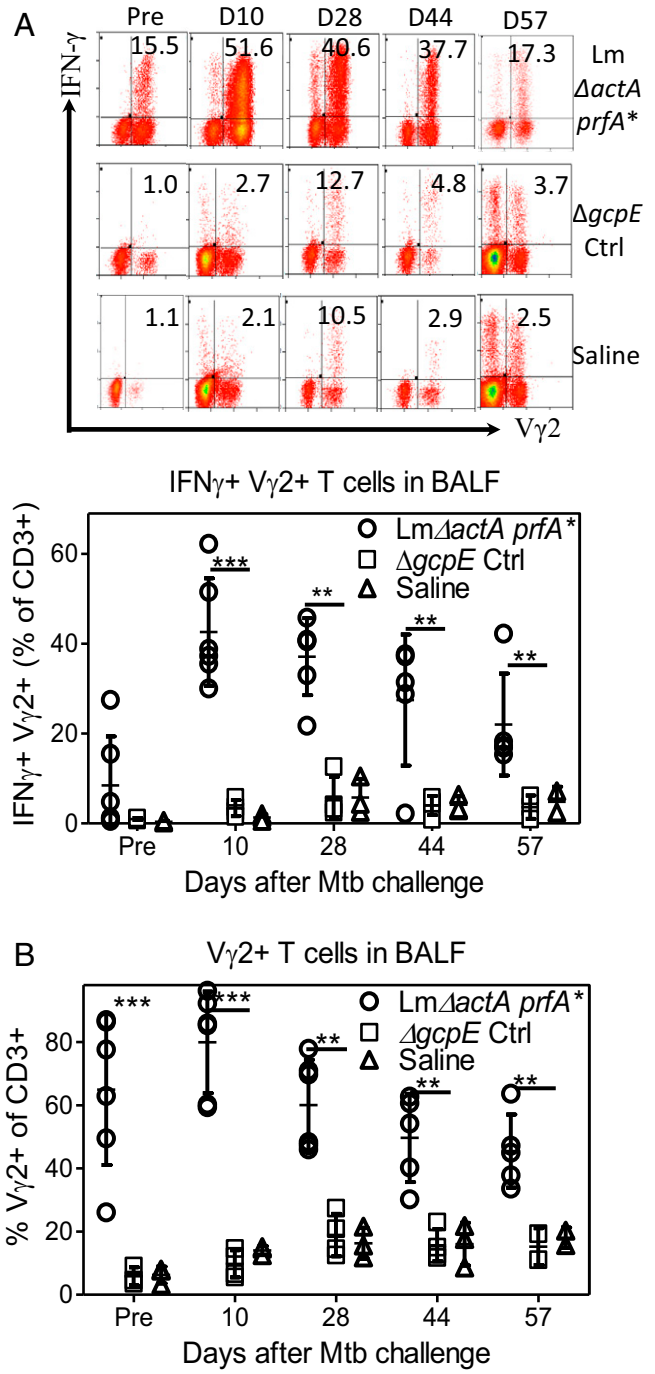

Fig. 4. Rapid and sustained increases in Th1-like Vγ2Vδ2 T cells in lungs after Mtb challenge of Lm *ΔactA prfA**-vaccinated macaques. (*A*) Representative flow cytometry histograms (*Upper*) and a graph (*Lower*) show percentages of IFN-γ^+ Vγ2^+ T cells in $CD3^+$ T cells in BAL fluid samples collected after 80-cfu Mtb challenge of the three groups vaccinated with Lm *ΔactA prfA** (*Top*), control (Ctrl) *ΔgcpE* (*Middle*), or saline (*Bottom*). The graph data are dot plots representing values for individual macaques in each group, and are derived from direct ICS assay without HMBPP stimulation in culture. (*B*) Graph dot plots showing percentages of Vγ2^+ T cells in $CD3^+$ T cells in BAL fluid samples from individual macaques of three indicated groups. $^{**}P < 0.01$; $^{***}P < 0.001$ (Mann–Whitney *U* test and ANOVA).

the lungs. At 10 d after Mtb challenge, CD4 Th1 cells in the airway increased to ∼10% of total $CD4^+$ cells and were maintained at 3–7% at later time points in Lm *ΔactA prfA**-vaccinated animals (Fig. 6*A* and *SI Appendix*, Fig. S5). In contrast, vector and saline control rhesus macaque groups had <1% of $CD4^+$ Th1 cells in the airway at most time points after the challenge (Fig. 6*A* and *SI Appendix*, Fig. S5). Concurrently, percentages of $CD8^+$ Th1-like cells in the lungs were also significantly greater in the Lm *ΔactA prfA**-vaccinated group compared with control groups (Fig. 6*B*). Of note, γδ T cell-associated increases in $CD4^+$ and $CD8^+$ Th1 cells after Mtb challenge were seen only in the airway, as there were no differences in frequencies of $CD4^+$ or $CD8^+$ Th1 cells in the blood between groups after Mtb challenge with or without in vitro restimulation with purified protein derivative (PPD).

Discussion

The current study reports that a single respiratory vaccination targeting the TB-reactive Vγ2Vδ2 T cell subset without concurrent immunization of Mtb-specific conventional αβ T cells can generate prolonged expansion of HMBPP-specific Vγ2Vδ2 T cells. This is associated with expression of their fast-acting capability to mount a rapid recall Th1-like effector response to Mtb challenge, and thereafter reduce Mtb infection. In previous studies, we employed two innovative "gain-of-function" manipulations, namely, HMBPP/IL-2 in vivo expansion and adoptive transfer of Vγ2Vδ2 T cells, and showed that Vγ2Vδ2 T cells can attenuate high-dose (500 cfu) Mtb infection in cynomolgus macaques (30, 33, 42). Here, in a proof-of-concept vaccine study, we showed that a single respiratory immunization of Vγ2Vδ2 T cells reduced Mtb infection and pathology after challenge with a moderate–high Mtb dose (80 cfu) in rhesus macaques.

Vaccine effects also coincide with tissue-resident Vγ2Vδ2 effector T cells that can coproduce IFN-γ and perforin and inhibit intracellular Mtb growth. The ability of vaccine-elicited Vγ2Vδ2 T cells to coproduce IFN-γ and perforin is consistent with earlier reports that Vγ2Vδ2 T cells have the pleiotropic capability to produce multiple cytokines (30, 42, 59). The correlation between anti-TB immunity and coproduction by γδ T cells of IFN-γ and perforin was consistent with the earlier observation that both IFN-γ and perforin are involved in the ability of Vγ2Vδ2 T effector cells to inhibit intracellular Mtb growth (30, 42). It has also been reported that Vγ2Vδ2 T cells producing other cytolytic effector molecules, including granulysin or granzyme A, can inhibit intracellular Mtb growth (60, 61).

Rapid recall expansion of IFN-γ^+ Vγ2Vδ2 T cells after Mtb challenge of Lm *ΔactA prfA**-vaccinated macaques coincided with accelerated pulmonary $CD4^+$ and $CD8^+$ Th1-like effector responses. Although the mechanism for this remains to be established, we speculate that Lm *ΔactA prfA**-elicited Vγ2Vδ2 T cells and the cytokines they produced during immunization might have primed or activated these antigen-specific $CD4^+$ and $CD8^+$ T cell subpopulations. In addition, the remarkable recall expansion of Vγ2Vδ2 T cells after Mtb infection likely provided further "helper" function enabling these activated $CD4^+$ and $CD8^+$ precursors to differentiate into IFN-γ^+ Th1-like effectors. This notion explains why there was a lack of apparent $CD4^+$ or $CD8^+$ Th1 responses before Mtb challenge of Lm *ΔactA prfA**-vaccinated macaques (Fig. 6 and *SI Appendix*, Fig. S5). Our findings suggest that rapid pulmonary Th1 responses of $CD4^+$ and $CD8^+$ T cells after respiratory immunization of Vγ2Vδ2 T cells may contribute to the vaccine-induced reduction of Mtb infection after challenge.

Establishing the concept of protective recall responses to Mtb by selective Vγ2Vδ2 T cell vaccines may help to open a new avenue for vaccine design. It is important to note that the HMBPP-specific Vγ2Vδ2 T cell subset exists only in primates, in which it constitutes 65–90% of total circulating γδ T cells in human adults. It is also noteworthy that in the 30 y that have elapsed since discovery of γδ T cells, the potential protective nature and vaccine utility of the human Vγ2Vδ2 T cell subset have not been defined. Further studies extending our findings in

MICROBIOLOGY

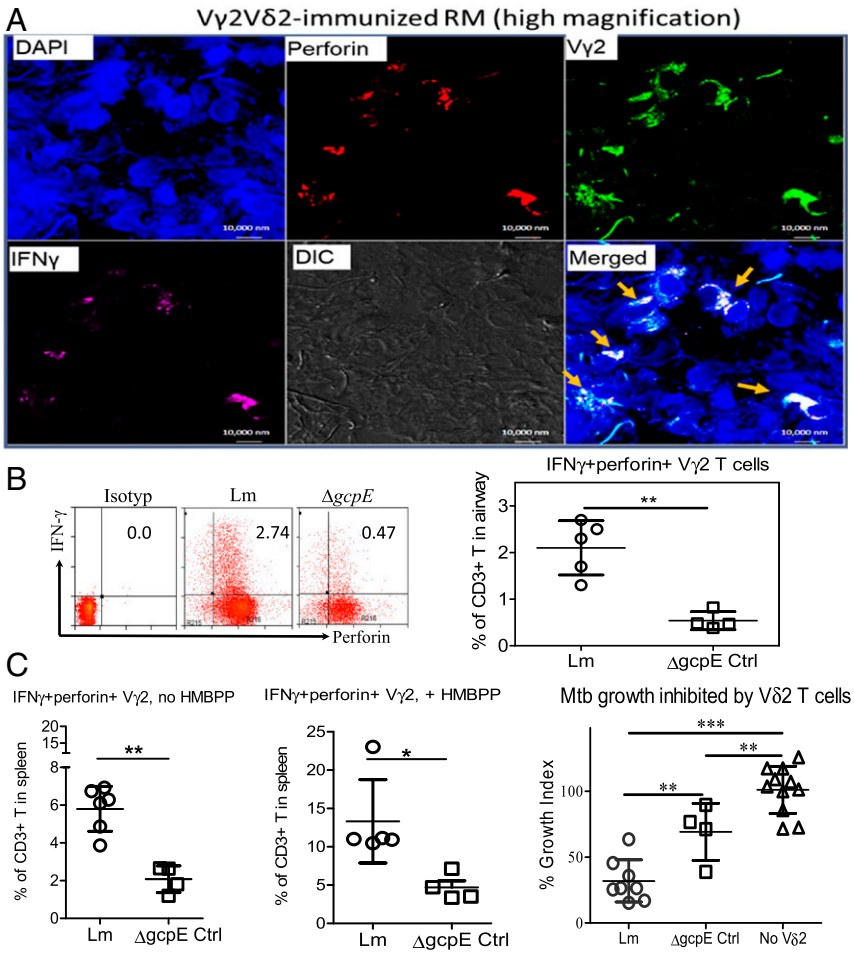

Fig. 5. Vaccine-induced reduction of TB infection coincides with tissue-resident Vγ2Vδ2 T effector cells coproducing IFN-γ and perforin and inhibiting intracellular Mtb growth. (*A*) Representative high-magnification photographs of in situ confocal microscopic images displaying lung resident Vγ2 (green) T effector cells that coexpress IFN-γ (pink) and perforin (red) in the merged images (colocalization marked by arrows) in tissue sections of the right caudal lung lobe from the test group receiving Lm *ΔactA prfA** immunization. Additional results are shown in *SI Appendix*, Fig. S4. In contrast, only a few IFN-γ^+ perforin$^+$ V$\gamma2^+$ cells were seen in the right caudal lung section from the control macaques (*SI Appendix*, Fig. S4). IgG isotype controls did not give detectable staining in TB-infected lung tissue sections (*SI Appendix*, Fig. S4). (*B*) Representative flow cytometry histograms (*Left*) and a graph (*Right*) show percentages of IFN-γ^+ perforin$^+$ Vγ2 T cells in CD3$^+$ T cells in BAL fluid samples collected at the end point from individual macaques in each group. The graph data are dot plots representing values with means ± SD for individual macaques in each group, and are derived from direct ICS assay without HMBPP stimulation in culture. Ctrl, control. (*C*, *Left* and *Center*) Dot plots representing percentages of IFN-γ^+ perforin$^+$ Vγ2 T cells in CD3$^+$ T cells from spleens of individual macaques in the indicated groups. Data are measured by direct ICS (*Left*, no HMBPP) and conventional ICS after HMBPP stimulation (*Center*, +HMBPP), respectively. (*C*, *Right*) Vδ2 T cells purified from spleens of Lm *ΔactA prfA**-vaccinated macaques exhibit stronger inhibition of Mtb growth in MΦ than those of *ΔgcpE* vector control animals. Anti-Vδ2 mAb (15D) worked readily for purification of Vγ2Vδ2 T cells. Data are dot plots with means ± SD for individual macaques in each group, and are expressed as a growth index (*Materials and Methods*), compared with MΦ alone without effector cells (No Vδ2) in culture. *$P < 0.05$; **$P < 0.01$; ***$P < 0.001$ (Mann–Whitney *U* test and ANOVA).

NHPs will provide an opportunity to close this long-standing knowledge gap. We previously demonstrated protective mechanisms by which CD4$^+$ and CD8$^+$ T cell populations protect against TB infection in primate models (56, 62, 63). The data presented in the current study support the view that TB vaccine design should include approaches to stimulate and expand the dominant Vγ2Vδ2 T cell subset, and support the feasibility and utility of inhaled Lm *ΔactA prfA** immunization as an approach to capture the potential of these cells for improving TB vaccines.

Materials and Methods

Macaque Animals and Institutional Animal Care and Use Committee Approval. Female and male rhesus macaques aged 4–8 y were used in the current study. All macaques had negative routine PPD TB test results. The use of macaques and all experimental procedures were approved by Institutional Animal Care and Use Committee and Biosafety Committees at University of Illinois at Chicago.

Vaccine Vector and Mtb Strains. Attenuated Lm strain Lm *ΔactA prfA** was originally obtained from Nancy Freitag, University of Illinois at Chicago, Chicago, as previously described (26). This strain carries the *gcpE* gene encoding the enzyme producing HMBPP. We developed and reported the *ΔgcpE* deletion mutant of Lm *ΔactA prfA*, which no longer produces HMBPP (31, 44, 48). The Mtb Erdman strain was used for bronchoscope-guided challenge or infection of macaques. The H37Rv strain was used for in vitro intracellular inhibition of Mtb growth in macrophages.

Respiratory Vaccination with Lm Strains. A total of 10^8 cfu of Lm *ΔactA prfA** or the *ΔgcpE* mutant was administered through intratracheal inoculation to Chinese-origin rhesus macaques (six per group), as previously described (48). Macaques were sedated with ketamine (10 mg/kg) and xylazine (1–2 mg/kg) by i.m. injection. An endotracheal tube was inserted through the larynx into the trachea and placed at the carina, and a 1-mL solution containing the inoculum was administered through the endotracheal tube. A 5-mL air bolus was administered through the tube following the inoculum to ensure the entire solution was given.

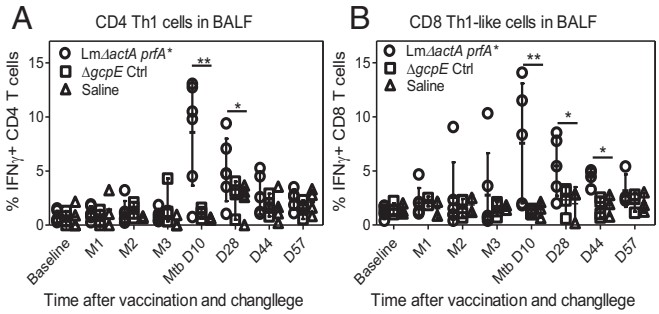

Fig. 6. Rapid pulmonary Th1 responses to Mtb challenge in Lm *ΔactA prfA**-immunized macaques. Graphs show frequencies of IFN-γ^+ CD4$^+$ Th1-like (*A*) and IFN-γ^+ CD8$^+$ Th1-like (*B*) effector cells in BAL fluid (BALF) samples from individual macaques in each group in the period from vaccination through the indicated end points after Mtb challenge. Shown in graphs are dot plots representing values with means ± SD for individual macaques; data are derived from direct ICS assay without antigen stimulation in the culture. $*P < 0.05$; $**P < 0.01$ (Mann–Whitney *U* test and ANOVA). Ctrl, control; D, day; M, month.

BAL and Isolation of Lymphocytes and PBMCs. Following sedation of macaques with ketamine and xylazine, BAL and fluid collection were carried out using a pediatric bronchoscope as previously described (42, 48), The bronchoscope was inserted into the bronchial branches distributing to the infected right caudal and other lung lobes of the animals to allow for harvesting of cells, including lymphocytes, in the airway. Isolation of lymphocytes from BAL fluid or the spleen and PBMCs from EDTA blood was done as previously described (32).

Phenotyping of PBMCs and BAL Lymphocytes. Cell surface markers on PBMCs and BAL fluid cells were analyzed by flow cytometry using fluorochrome-conjugated antibodies as previously described (51). Cells were incubated with antibodies against cell surface markers for 15 min. Cells were washed and fixed with 2% formalin and analyzed on an LSR Fortessa flow cytometer (BD Biosciences).

ICS. Analysis of cytokine production following antigen restimulation ex vivo was done using previously described methods (51). We also used direct ICS to assess limited BAL cells or PBMCs for intracellular cytokines without prior in vitro Ag stimulation. Direct ICS was previously validated and described (32, 49, 51, 53, 52). Details are provided in *SI Appendix*.

Intracellular Mtb Growth Inhibition Assay. The extent of inhibition of Mtb growth in autologous monocyte-derived macrophages by Vδ2 T cells was assayed using a modification of the previously described method (30, 42) (*SI Appendix*). Inhibition data were expressed as a growth index (colony-forming unit counts of monocytes plus effector cells/colony-forming unit counts of monocytes alone) as described (64).

Mtb Infection of Rhesus Macaques. Macaques were sedated with ketamine (10 mg/kg) and xylazine (1–2 mg/kg) by i.m. injection. A pediatric bronchoscope was inserted into the right caudal lung lobe of the animals, and 80 cfu of Mtb Erdman strain was injected in 3 mL of saline followed by a 3-mL bolus of air to ensure full dose administration. The colony-forming unit dose for infection was confirmed by careful postinoculation titration on a Middlebrook 7H11 plate (Becton Dickinson) as previously described (52).

Determination of Tissue Bacterial Loads. Tissues were harvested and processed for Mtb colony-forming unit determination as described previously (30, 42, 52) and in *SI Appendix*. Briefly, tissue homogenates were made using a homogenizer (PRO 200; PRO Scientific) and were diluted using sterile PBS + 0.05% Tween-80. Fivefold serial dilutions of samples were plated on Middlebrook 7H11 plates. The colony-forming unit counts on plates were measured after 3–4 wk of culture.

Macroscopic and Microscopic Pathological Analysis of TB Lesions. Details are described in previous studies (30, 42, 52) and *SI Appendix*. Multiple tissue specimens were collected from all organs whether or not they showed gross lesions. For organs with visible lesions, their number, location, size, distribution, and consistency were recorded. A standard scoring system was used to calculate gross pathology scores for TB lesions (30, 42, 52), and all scorings were performed in a blinded fashion. Microscopic pathological analysis was done essentially the same as described elsewhere (30, 42, 52).

Statistical Analysis. Statistical analysis was done using a paired *t* test or Mann–Whitney *U* test or ANOVA as indicated. $P < 0.05$ was considered significant. All statistical analyses were conducted using GraphPad software (Prism).

ACKNOWLEDGMENTS. The current work is an extension of decades-long seminal γδ T cell studies. W.R.J. has had a direct role in the design and execution of a significant fraction of the current studies. The subject matter is within the area of expertise of W.R.J. This work was supported by National Institutes of Health Grants R01OD015092, 2018ZX10731301-006-001, R01HL064560, R01HL129887, R01AI26170, and P01AI063537.

1. GBD 2016 Causes of Death Collaborators (2017) Global, regional, and national age-sex specific mortality for 264 causes of death, 1980-2016: A systematic analysis for the Global Burden of Disease Study 2016. *Lancet* 390:1151–1210.
2. Murray CJ, et al. (2014) Global, regional, and national incidence and mortality for HIV, tuberculosis, and malaria during 1990-2013: A systematic analysis for the Global Burden of Disease Study 2013. *Lancet* 384:1005–1070.
3. Wells CD, et al. (2007) HIV infection and multidrug-resistant tuberculosis: The perfect storm. *J Infect Dis* 196(Suppl 1):S86–S107.
4. Lawn SD, Zumla AI (2011) Tuberculosis. *Lancet* 378:57–72.
5. Dockrell HM, Smith SG (2017) What have we learnt about BCG vaccination in the last 20 years? *Front Immunol* 8:1134.
6. Colditz GA, et al. (1994) Efficacy of BCG vaccine in the prevention of tuberculosis. Meta-analysis of the published literature. *JAMA* 271:698–702.
7. Kaufmann SHE, Gengenbacher M (2012) Recombinant live vaccine candidates against tuberculosis. *Curr Opin Biotechnol* 23:900–907.
8. Rodrigues LC, Diwan VK, Wheeler JG (1993) Protective effect of BCG against tuberculous meningitis and miliary tuberculosis: A meta-analysis. *Int J Epidemiol* 22: 1154–1158.
9. Trunz BB, Fine P, Dye C (2006) Effect of BCG vaccination on childhood tuberculous meningitis and miliary tuberculosis worldwide: A meta-analysis and assessment of cost-effectiveness. *Lancet* 367:1173–1180.
10. Yuk J-M, Jo E-K (2014) Host immune responses to mycobacterial antigens and their implications for the development of a vaccine to control tuberculosis. *Clin Exp Vaccine Res* 3:155–167.
11. Verreck FAW, et al. (2017) Variable BCG efficacy in rhesus populations: Pulmonary BCG provides protection where standard intra-dermal vaccination fails. *Tuberculosis (Edinb)* 104:46–57.
12. Nieuwenhuizen NE, Kaufmann SHE (2018) Next-generation vaccines based on bacille Calmette-Guérin. *Front Immunol* 9:121.
13. Tameris MD, et al.; MVA85A 020 Trial Study Team (2013) Safety and efficacy of MVA85A, a new tuberculosis vaccine, in infants previously vaccinated with BCG: A randomised, placebo-controlled phase 2b trial. *Lancet* 381:1021–1028.
14. Nemes E, et al.; C-040-404 Study Team (2018) Prevention of M. tuberculosis infection with H4:IC31 vaccine or BCG revaccination. *N Engl J Med* 379:138–149.
15. Van Der Meeren O, et al. (2018) Phase 2b controlled trial of M72/AS01$_E$ vaccine to prevent tuberculosis. *New Engl J Med* 379:1621–1634.
16. Kaufmann SHE, et al.; TBVAC2020 Consortium (2017) TBVAC2020: Advancing tuberculosis vaccines from discovery to clinical development. *Front Immunol* 8:1203.
17. Hansen SG, et al. (2018) Prevention of tuberculosis in rhesus macaques by a cytomegalovirus-based vaccine. *Nat Med* 24:130–143.
18. Darrah PA, et al. (2014) Aerosol vaccination with AERAS-402 elicits robust cellular immune responses in the lungs of rhesus macaques but fails to protect against high-dose Mycobacterium tuberculosis challenge. *J Immunol* 193:1799–1811.
19. Lin PL, et al. (2012) The multistage vaccine H56 boosts the effects of BCG to protect cynomolgus macaques against active tuberculosis and reactivation of latent Mycobacterium tuberculosis infection. *J Clin Invest* 122:303–314.
20. Jeyanathan M, et al. (2015) AdHu5Ag85A respiratory mucosal boost immunization enhances protection against pulmonary tuberculosis in BCG-primed non-human primates. *PLoS One* 10:e0135009.
21. Bertholet S, et al. (2010) A defined tuberculosis vaccine candidate boosts BCG and protects against multidrug-resistant Mycobacterium tuberculosis. *Sci Transl Med* 2: 53ra74.
22. Kaushal D, et al. (2015) Mucosal vaccination with attenuated Mycobacterium tuberculosis induces strong central memory responses and protects against tuberculosis. *Nat Commun* 6:8533.
23. Laddy DJ, et al. (2018) Toward tuberculosis vaccine development: Recommendations for nonhuman primate study design. *Infect Immun* 86:e00776-17.
24. Voss G, et al. (2018) Progress and challenges in TB vaccine development. *F1000 Res* 7:199.
25. Perdomo C, et al. (2016) Mucosal BCG vaccination induces protective lung-resident memory T cell populations against tuberculosis. *MBio* 7:e01686-16.
26. Yin Y, et al. (2017) A promising listeria-vectored vaccine induces Th1-type immune responses and confers protection against tuberculosis. *Front Cell Infect Microbiol* 7:407.

27. Nielsen MM, Witherden DA, Havran WL (2017) γδ T cells in homeostasis and host defence of epithelial barrier tissues. *Nat Rev Immunol* 17:733–745.
28. Vantourout P, Hayday A (2013) Six-of-the-best: Unique contributions of γδ T cells to immunology. *Nat Rev Immunol* 13:88–100.
29. Shen Y, et al. (2002) Adaptive immune response of Vgamma2Vdelta2+ T cells during mycobacterial infections. *Science* 295:2255–2258.
30. Chen CY, et al. (2013) Phosphoantigen/IL2 expansion and differentiation of Vγ2Vδ2 T cells increase resistance to tuberculosis in nonhuman primates. *PLoS Pathog* 9: e1003501.
31. Ryan-Payseur B, et al. (2012) Multieffector-functional immune responses of HMBPP-specific Vγ2Vδ2 T cells in nonhuman primates inoculated with Listeria monocytogenes ΔactA prfA*. *J Immunol* 189:1285–1293.
32. Yao S, et al. (2010) Differentiation, distribution and gammadelta T cell-driven regulation of IL-22-producing T cells in tuberculosis. *PLoS Pathog* 6:e1000789.
33. Huang D, et al. (2009) Antigen-specific Vgamma2Vdelta2 T effector cells confer homeostatic protection against pneumonic plaque lesions. *Proc Natl Acad Sci USA* 106: 7553–7558.
34. Belmant C, et al. (1999) 3-Formyl-1-butyl pyrophosphate A novel mycobacterial metabolite-activating human gammadelta T cells. *J Biol Chem* 274:32079–32084.
35. Eberl M, et al. (2003) Microbial isoprenoid biosynthesis and human gammadelta T cell activation. *FEBS Lett* 544:4–10.
36. Bonneville M, O'Brien RL, Born WK (2010) Gammadelta T cell effector functions: A blend of innate programming and acquired plasticity. *Nat Rev Immunol* 10:467–478.
37. Chen ZW (2011) Immune biology of Ag-specific γδ T cells in infections. *Cell Mol Life Sci* 68:2409–2417.
38. Davey MS, et al. (2011) Human neutrophil clearance of bacterial pathogens triggers anti-microbial γδ T cell responses in early infection. *PLoS Pathog* 7:e1002040.
39. Meraviglia S, Caccamo N, Salerno A, Sireci G, Dieli F (2010) Partial and ineffective activation of V gamma 9V delta 2 T cells by Mycobacterium tuberculosis-infected dendritic cells. *J Immunol* 185:1770–1776.
40. Gong G, et al. (2009) Phosphoantigen-activated V gamma 2V delta 2 T cells antagonize IL-2-induced CD4+CD25+Foxp3+ T regulatory cells in mycobacterial infection. *Blood* 113:837–845.
41. Ali Z, et al. (2007) Prolonged (E)-4-hydroxy-3-methyl-but-2-enyl pyrophosphate-driven antimicrobial and cytotoxic responses of pulmonary and systemic Vgamma2Vdelta2 T cells in macaques. *J Immunol* 179:8287–8296.
42. Qaqish A, et al. (2017) Adoptive transfer of phosphoantigen-specific γδ T cell subset attenuates *Mycobacterium tuberculosis* infection in nonhuman primates. *J Immunol* 198:4753–4763.
43. Singh R, Paterson Y (2006) Listeria monocytogenes as a vector for tumor-associated antigens for cancer immunotherapy. *Expert Rev Vaccines* 5:541–552.
44. Yan L, et al. (2008) Selected prfA* mutations in recombinant attenuated Listeria monocytogenes strains augment expression of foreign immunogens and enhance vaccine-elicited humoral and cellular immune responses. *Infect Immun* 76:3439–3450.
45. Qiu J, et al. (2011) Intranasal vaccination with the recombinant Listeria monocytogenes ΔactA prfA* mutant elicits robust systemic and pulmonary cellular responses and secretory mucosal IgA. *Clin Vaccine Immunol* 18:640–646.
46. Shen H, et al. (2015) Th17-related cytokines contribute to recall-like expansion/effector function of HMBPP-specific Vγ2Vδ2 T cells after Mycobacterium tuberculosis infection or vaccination. *Eur J Immunol* 45:442–451.
47. Frencher JT, et al. (2013) SHIV antigen immunization alters patterns of immune responses to SHIV/malaria coinfection and protects against life-threatening SHIV-related malaria. *J Infect Dis* 208:260–270.
48. Frencher JT, et al. (2014) HMBPP-deficient Listeria mutant immunization alters pulmonary/systemic responses, effector functions, and memory polarization of Vγ2Vδ2 T cells. *J Leukoc Biol* 96:957–967.
49. Ryan-Payseur B, et al. (2011) Virus infection stages and distinct Th1 or Th17/Th22 T-cell responses in malaria/SHIV coinfection correlate with different outcomes of disease. *J Infect Dis* 204:1450–1462.
50. White AD, et al. (2015) Evaluation of the immunogenicity of Mycobacterium bovis BCG delivered by aerosol to the lungs of macaques. *Clin Vaccine Immunol* 22: 992–1003.
51. Ali Z, et al. (2009) γδ T cell immune manipulation during chronic phase of simian-HIV infection confers immunological benefits. *J Immunol* 183:5407–5417.
52. Chen CY, et al. (2012) IL-2 simultaneously expands Foxp3+ T regulatory and T effector cells and confers resistance to severe tuberculosis (TB): Implicative Treg-T effector cooperation in immunity to TB. *J Immunol* 188:4278–4288.
53. Zeng G, et al. (2011) Membrane-bound IL-22 after de novo production in tuberculosis and anti-Mycobacterium tuberculosis effector function of IL-22+ CD4+ T cells. *J Immunol* 187:190–199.
54. Maiello P, et al. (2018) Rhesus macaques are more susceptible to progressive tuberculosis than cynomolgus macaques: A quantitative comparison. *Infect Immun* 86: e00505-17.
55. Qiu L, et al. (2008) Severe tuberculosis induces unbalanced up-regulation of gene networks and overexpression of IL-22, MIP-1alpha, CCL27, IP-10, CCR4, CCR5, CXCR3, PD1, PDL2, IL-3, IFN-beta, TIM1, and TLR2 but low antigen-specific cellular responses. *J Infect Dis* 198:1514–1519.
56. Chen CY, et al. (2009) A critical role for CD8 T cells in a nonhuman primate model of tuberculosis. *PLoS Pathog* 5:e1000392.
57. Huang D, et al. (2008) Immune distribution and localization of phosphoantigen-specific Vgamma2Vdelta2 T cells in lymphoid and nonlymphoid tissues in Mycobacterium tuberculosis infection. *Infect Immun* 76:426–436.
58. Chen ZW (2013) Multifunctional immune responses of HMBPP-specific Vγ2Vδ2 T cells in M. tuberculosis and other infections. *Cell Mol Immunol* 10:58–64.
59. Vermijlen D, et al. (2007) Distinct cytokine-driven responses of activated blood gammadelta T cells: Insights into unconventional T cell pleiotropy. *J Immunol* 178: 4304–4314.
60. Spencer CT, et al. (2013) Granzyme A produced by γ(9)δ(2) T cells induces human macrophages to inhibit growth of an intracellular pathogen. *PLoS Pathog* 9: e1003119.
61. Dieli F, et al. (2001) Granulysin-dependent killing of intracellular and extracellular Mycobacterium tuberculosis by Vgamma9/Vdelta2 T lymphocytes. *J Infect Dis* 184: 1082–1085.
62. Yao S, et al. (2014) CD4+ T cells contain early extrapulmonary tuberculosis (TB) dissemination and rapid TB progression and sustain multieffector functions of CD8+ T and CD3- lymphocytes: Mechanisms of CD4+ T cell immunity. *J Immunol* 192: 2120–2132.
63. Du G, et al. (2010) TCR repertoire, clonal dominance, and pulmonary trafficking of mycobacterium-specific CD4+ and CD8+ T effector cells in immunity against tuberculosis. *J Immunol* 185:3940–3947.
64. Yang R, et al. (2018) IL-12+IL-18 cosignaling in human macrophages and lung epithelial cells activates cathelicidin and autophagy, inhibiting intracellular mycobacterial growth. *J Immunol* 200:2405–2417.